

# Enhanced quantum teleportation in non-Markovian environments

Xiang Hao

*Department of Physics, School of Mathematics and Physics,  
Suzhou University of Science and Technology,  
Suzhou, Jiangsu 215011, People's Republic of China*

Shiqun Zhu\*

*School of Physical Science and Technology, Suzhou University,  
Suzhou, Jiangsu 215006, People's Republic of China*

## Abstract

The protocol of the teleportation of an arbitrary unknown one-qubit state is investigated when the quantum channel is subject to the decoherence from the non-Markovian environments with the memory effects. The quality of the teleportation measured by the average fidelity and minimal fidelity can be enhanced in the non-Markovian channel. The memory effects give rise to the revival of the fidelity which is better than that obtained by the Markovian channel.

Keywords: quantum teleportation, non-Markovian dynamics, average fidelity

PACS: 03.67.Hk, 03.65.Ud

---

\*Corresponding author; Electronic address: szhu@suda.edu.cn

## I. INTRODUCTION

The realistic quantum systems[1, 2] are usually open to environments which result in the uncontrollable decoherence and dissipation[3, 4]. Therefore, it is of great importance to study the impacts of environments on the feasible quantum information processing such as quantum teleportation [5–9]. Quantum teleportation is the protocol which enables the recreation of an arbitrary unknown state at a remote place via the local measurements and necessary classical communications. The key to the standard teleportation is entangled states acting as the quantum channel. Recently, some schemes via the noisy channel of the mixed states have been extensively studied in [10–19]. These investigations reveal an interesting point that the entanglement of the channel mainly influences the quality of the teleportation. The effects of the environments have also been taken into account. The previous results of the above works manifest that the type of noises acting on the quantum channel can determine the efficiency of the teleportation. If the fidelity is smaller than the critical value of  $2/3$ , the entanglement of the channel will be decreased to zero. These noises are considered in the Markovian limit with the assumption of an infinitely short correlation time of the environment. However, the conventionally employed Markovian approximation has faced more and more challenges because of the rapid advance of experimental techniques[3]. Recent studies have shown that non-Markovian quantum processes play an increasingly important role in many fields of physics [20–26]. The apparent feature of the non-Markovian dynamics is the memory effects from the practical environment with a certain correlation time. To quantitatively characterize the memory effect, some measures for the degrees of the non-Markovianity have been introduced by [27–29]. These reasons motivate us to investigate how non-Markovian environments influence a protocol of quantum teleportation.

In this paper, we consider a general mixed two-qubit states as the noisy channel coupled to two local non-Markovian reservoirs. The non-Markovian dynamics of the average fidelity of the teleportation is derived. For the long time limit, we use the minimal fidelity to quantify the success of the teleportation protocol. Finally, a simple conclusion is given.

## II. THE FORMALISM

In the following discussion, we investigate the quantum teleportation in the noisy channel which is composed of the two noninteracting parts. For each part, a qubit  $S = A, B$  is locally coupled to a reservoir  $R_S = R_A, R_B$  with the memory effects. The Hamiltonian of the quantum channel is described by

$$H^c = \sum_{S=A,B} H_S^0 + H_{R_S}^0 + H_{S,R_S}^I. \quad (1)$$

The inherent Hamiltonian of each qubit  $S$  is formed by  $H_S^0 = \omega_0 \sigma_+^S \sigma_-^S$  where  $\omega_0$  is the transition frequency of the effective two-level system with the excited state  $|e\rangle_S$  and ground state  $|g\rangle_S$ .  $\sigma_{\pm}^S$  denotes the raising and lowering operators respectively. The local reservoir is given by the  $H_{R_S}^0 = \sum_j \omega_j b_{R_S,j}^+ b_{R_S,j}$  where the index  $j$  labels the field mode of the reservoir with the corresponding frequency  $\omega_j$ .  $b_{R_S,j}^+, b_{R_S,j}$  are the creation and annihilation operators of the mode for the reservoir  $R_S$ . The qubit-reservoir interaction Hamiltonian is also obtained by  $H_{S,R_S}^I = \sigma_+^S B_{R_S} + \sigma_-^S B_{R_S}^+$  where  $B_{R_S} = \sum_j g_{R_S,j} b_{R_S,j}$  and  $g_{R_S,j}$  represents the coupling between the qubit and the reservoir.

We suppose that the qubits of the channel are initially prepared in a general mixed states  $\rho^c(0)$  which can be expressed in the standard product basis  $\{|1\rangle = |ee\rangle, |2\rangle = |eg\rangle, |3\rangle = |ge\rangle, |4\rangle = |gg\rangle\}$ . The elements of the density matrix satisfy that  $\sum_{n=1}^4 \rho_{nn}^c(0) = 1$  and  $\rho_{mn}^c(0) = [\rho_{nm}^c(0)]^*$ . If the dynamical map  $\varepsilon_S$  for each qubit is known, the evolution of the states for the quantum channel can be obtained by

$$\rho^c(t) = \varepsilon_A \otimes \varepsilon_B[\rho^c(0)]. \quad (2)$$

In accordance with the result of [3], the non-Markovian dynamics  $\varepsilon_S$  can be written as

$$\begin{aligned} \varepsilon_S(|e\rangle\langle e|) &= |G_S(t)|^2 |e\rangle\langle e| + [1 - |G_S(t)|^2] |g\rangle\langle g| \\ \varepsilon_S(|e\rangle\langle g|) &= G_S(t) |e\rangle\langle g| \\ \varepsilon_S(|g\rangle\langle e|) &= G_S^*(t) |g\rangle\langle e| \\ \varepsilon_S(|g\rangle\langle g|) &= |g\rangle\langle g|, \end{aligned} \quad (3)$$

where each local reservoir is initially in the vacuum state and the function  $G_S(t) = G(t)$  is defined as the solution of the integrodifferential equation

$$\dot{G}(t) = - \int_0^t f(t-\tau) G(\tau) d\tau. \quad (4)$$

The two-point reservoir correlation function  $f(t - \tau)$  is closely related to the spectral density of the reservoir  $J(\omega)$ ,  $f(t - \tau) = \int J(\omega) \exp[i(\omega_0 - \omega)(t - \tau)] d\omega$ . For example, we take the detuning case of the Lorentzian spectral density which describes the vacuum radiation field inside an imperfect cavity [3],

$$J(\omega) = \frac{1}{\pi} \frac{W^2 \lambda}{(\omega_0 - \omega - \delta)^2 + \lambda^2}, \quad (5)$$

where  $\delta = \omega_0 - \omega_c$  is the detuning between the center frequency of the cavity  $\omega_c$  and the resonance frequency  $\omega_0$ .  $W$  represents the interaction strength between the qubit and its local reservoir. The parameter  $\lambda$  defines the spectral width of the reservoir. It is found out that the effective coupling between the qubit and local reservoir is dependent on the detuning [3]. The large values of  $\delta$  represent the weak effective couplings [3]. This also means that the effects of the reservoirs on the protocol are small when the detuning  $\delta$  is increased. We can verify that the correlation function decays exponentially  $f(t - \tau) = W^2 \exp[-(\lambda - i\delta)(t - \tau)]$ . The correlation time scale of the reservoir is approximately estimated by  $\tau_R \sim \lambda^{-1}$ . As another necessary time parameter, the relaxation time for each qubit is also obtained by  $\tau_S \sim \gamma_0^{-1}$  where  $\gamma_0 = 2W^2/\lambda$  is regarded as the decaying rate of the qubit in the Markovian limit of flat spectrum. Applying the correlation function  $f(t - \tau)$ , we can obtain the expression of  $G(t)$ ,

$$G(t) = \exp[-\frac{1}{2}(\lambda - i\delta)t] (\cosh \frac{dt}{2} + \frac{\lambda - i\delta}{d} \sinh \frac{dt}{2}), \quad (6)$$

with  $d = \sqrt{(\lambda - i\delta)^2 - 2\gamma_0\lambda}$ . If the time scale  $\tau_R$  is comparable with the relaxation time scale  $\tau_S$ , i.e.,  $\tau_R > \tau_S/2$ , the memory effects of the reservoir should be taken into account. When  $\lambda \ll \gamma_0$  and  $\delta = 0$ , the function is simplified as  $G(t) = e^{-\frac{\lambda t}{2}} (\cos \frac{d|t}{2} + \frac{\lambda}{d} \sin \frac{d|t}{2})$ . It is clearly seen that the revivals of  $G(t)$  occur in this case. While  $\tau_R \ll \tau_S$  or  $\lambda \gg \gamma_0$ , the dynamical map reduces to the Markovian decoherence where  $|G(t)| = e^{-\frac{\gamma_0 t}{2}}$  is monotonically decreasing with time.

### III. TELEPORTATION IN THE ENVIRONMENTS

Without the loss of the generality, an arbitrary unknown single qubit state  $|\varphi_{in}\rangle = \cos \frac{\theta}{2} |e\rangle + \sin \frac{\theta}{2} e^{i\phi} |g\rangle$  is recognized as one input state for the standard teleportation. The parameter  $\theta \in [0, \pi]$  and  $\phi \in [0, 2\pi]$  represent the polar and azimuthal angles respectively. The protocol uses a shared quantum state as a quantum channel to transfer a third quantum

state between two distant parties. For a stationary quantum channel, quantum teleportation can be performed when the parties  $A$  and  $B$  can determine which Bell state has the largest overlap with the quantum channel. When the quantum channel varies with time, the optimal Bell state will possibly change after the time  $T$ . In that time, the quantum channel has evolved to  $\rho_c(T)$ . If the parties  $A$  and  $B$  have complete knowledge of the evolution process, they will be able to correctly select the optimal Bell state. According to the work of [13], the definite expression of the output state  $\rho_{out}^{(m)}(T)$  can be written as

$$\rho_{out}^{(m)}(T) = \sum_{j=0}^3 p_j^{(m)}(T) \sigma_j \rho_{in} \sigma_j, \quad (7)$$

where the local operations  $\sigma_j (j = 1, 2, 3)$  are the three components of the Pauli rotation,  $\sigma_0 = I$  denotes the unity matrix and  $\rho_{in} = |\varphi_{in}\rangle\langle\varphi_{in}|$ . The probabilities  $p_j^{(m)} = \langle\Psi^{(j\oplus m)}|\rho^c(t)|\Psi^{(j\oplus m)}\rangle = \text{Tr}[\rho_{Bell}^{(j\oplus m)}\rho^c(t)]$  satisfying that  $\sum_{j=0}^3 p_j^{(m)} = 1$ . Although the form of Eq. (7) is different from the result of [7, 8], all of the expressions discover the fact that the teleportation via the channel of mixed states is equivalent to a generalized depolarizing channel with the probabilities obtained by the maximally entangled components of the channel. It is noted that the values of  $m$  are time dependent. Here  $j \oplus m (m = 0, 1, 2, 3)$  represents summation modulus 4 and  $\rho_{Bell}^{(j\oplus m)} = |\Psi^{(j\oplus m)}\rangle\langle\Psi^{(j\oplus m)}|$  describes the density matrix of the four Bell entangled states  $\{|\Psi^{(0,3)}\rangle = \frac{1}{\sqrt{2}}(|ee\rangle \pm |gg\rangle), |\Psi^{(1,2)}\rangle = \frac{1}{\sqrt{2}}(|eg\rangle \pm |ge\rangle)\}$ . The above equation describes the output state through the channel with the maximally entangled fraction  $|\Psi^{(m)}\rangle$  after the implementation of Bell measurements and corresponding pauli operations.

In regard to the environments, the maximally entangled component of the noisy channel can be varied with time. Therefore, the best quality of the teleportation can be obtained by the optimal estimation of the four possible output states. To efficiently measure the quality of the protocol, the average fidelity between the input state and output one can be written as  $F^{(m)} = \frac{1}{4\pi} \int_0^{2\pi} \int_0^\pi \langle\varphi_{in}|\rho_{out}^{(m)}|\varphi_{in}\rangle \sin\theta d\theta d\phi$ . For a given noisy channel, we can optimize the standard teleportation by choosing certain values of  $m$  to maximize the average fidelity. The achievable maximum of the four average fidelity can be given by

$$F(t) = \frac{1}{3} + \frac{2}{3} \max_m \{p_0^{(m)}(t)\}, \quad (8)$$

where the probabilities  $p_0^{(m)}(t) = \langle\Psi^{(m)}|\rho^c(t)|\Psi^{(m)}\rangle$  are only connected with the diagonal and anti-diagonal elements of  $\rho^c(t)$ . The maximum of  $\{p_0^{(m)}(t), (m = 0, 1, 2, 3)\}$  can be obtained

as

$$\max_m \{p_0^{(m)}(t)\} = \frac{1}{2} \max\{\mu_1(t), \mu_2(t)\}, \quad (9)$$

where  $\mu_1(t) = \rho_{11}^c(t) + \rho_{44}^c(t) + 2|\text{Re}[\rho_{14}^c(t)]|$ ,  $\mu_2(t) = 1 - \rho_{44}^c(t) + 2|\text{Re}[\rho_{23}^c(t)]|$  and  $\text{Re}[a]$  denotes the real part of  $a$ . In this case, the diagonal elements of  $\rho^c(t)$  are

$$\begin{aligned} \rho_{11}^c(t) &= \rho_{11}^c(0)|G(t)|^4 \\ \rho_{22}^c(t) &= \rho_{11}^c(0)|G(t)|^2[1 - |G(t)|^2] + \rho_{22}^c(0)|G(t)|^2 \\ \rho_{33}^c(t) &= \rho_{11}^c(0)|G(t)|^2[1 - |G(t)|^2] + \rho_{33}^c(0)|G(t)|^2 \\ \rho_{44}^c(t) &= 1 - \rho_{11}^c(t) - \rho_{22}^c(t) - \rho_{33}^c(t), \end{aligned} \quad (10)$$

and the anti-diagonal elements are also given by

$$\begin{aligned} \rho_{14}^c(t) &= \rho_{14}^c(0)G^2(t) \\ \rho_{23}^c(t) &= \rho_{23}^c(0)|G(t)|^2. \end{aligned} \quad (11)$$

For simplicity, we can take the maximally entangled states to be the initial ones for the channel. When  $\rho^c(0) = |\Psi^{(0,3)}\rangle\langle\Psi^{(0,3)}|$ , the optimized average fidelity is obtained by

$$F(t) = \frac{1}{3}[2 + |G(t)|^4]. \quad (12)$$

During the decoherence, the probabilities  $|\Psi^{(0,3)}\rangle$  of the channel are always larger than those of  $|\Psi^{(1,2)}\rangle$ . Figures 1-4 show that the dynamics of the optimized average fidelity is dependent on the scaled time  $\gamma_0 t$  in the Markovian regime of  $\lambda = 5\gamma_0$  and non-Markovian regime of  $\lambda = 0.01\gamma_0$ . In Fig. 1, the values of  $F(t)$  are rapidly decreased to the critical value  $2/3$  below which the quality of the teleportation is worse than that of the classical communication. With the increasing of the detuning  $\delta$ , the decaying rate of the optimized average fidelity is smaller than that of the resonance case  $\delta = 0$ . In Fig. 2, the revivals of the average fidelity occur after a finite period time of  $F(t) = 2/3$  when  $\delta = 0$ . The large detuning of the reservoir can ensure the preservation of high values of the optimized average fidelity. This is the reason that the effective interactions between the qubits and reservoirs are weak when the detuning values  $\delta$  are large. For  $\rho^c(0) = |\Psi^{(1,2)}\rangle\langle\Psi^{(1,2)}|$ , the optimized average fidelity is expressed by

$$F(t) = \frac{1}{3} + \frac{1}{3} \max\{1 - |G(t)|^2, 2|G(t)|^2\}. \quad (13)$$

From Fig. 3, we can clearly see that the values of the optimized average fidelity are rapidly decreased to a certain value and then gradually increased to the critical value  $2/3$  in the Markovian case. Meanwhile, the similar revivals of the average fidelity also occur in Fig. 4 when the effects of the non-Markovian environment are considered. When the detuning is large, the high values of average fidelity can remain during the evolution. In this condition, it is noted that if the probability  $|\Psi^{(1,2)}\rangle$  of the channel is larger than  $|\Psi^{(0,3)}\rangle$ , the value of average fidelity  $F(t) > 2/3$ . This means that the purity of the channel state can affect the quality of the teleportation.

#### IV. THE MINIMAL FIDELITY FOR THE PROTOCOL

For the long time, the quantum channel is in the  $|gg\rangle$  state. The average fidelity in this case is  $2/3$ , even though the  $|gg\rangle$  state is nearly the worst quantum channel for teleportation. From this point of view, we may consider the minimal fidelity as a better measure to quantify the success of the teleportation protocol. The minimization can be performed over all possible values of  $\theta$  and  $\phi$ , i.e.,  $f(t) = \min_{\theta, \phi} \{ \langle \varphi_{in} | \rho_{out}^{(m)}(t) | \varphi_{in} \rangle \}$ . Figure 5 shows the minimal fidelity of the teleportation protocol when the initial entangled resource is chosen to be  $|\Psi^{(0,3)}\rangle$ . The minimal fidelity for  $\rho^c(0) = |\Psi^{(0,3)}\rangle\langle\Psi^{(0,3)}|$  can be obtained by,

$$f(t) = \frac{1}{2} + \frac{\text{Re}[G^2(t)]}{2}. \quad (14)$$

It is clearly seen that the revival of the fidelity is mainly dependent on the memory effect from the non-Markovian environment. For the time limit  $t \gg \frac{1}{\lambda}$ , the minimal fidelity for the initial channel of  $|\Psi^{(0,3)}\rangle$  is  $\frac{1}{2}$ . With increasing the detuning value  $\delta$ , the minimal fidelity can be greatly improved at the large time scale. This point demonstrates the memory effects from the non-Markovian environments can enhance the success of the teleportation protocol. When the initial channel state is  $|\Psi^{(1,2)}\rangle$ , the minimal fidelity is plotted in Figure 6. The analytical expression of  $f(t)$  in this case is given by,

$$f(t) = |G(t)|^2. \quad (15)$$

The revival of the fidelity for  $\delta = 0$  is clearly shown in Figure 6(a). If the detuning value is increased, the minimal fidelity can keep the high values for a long time. The large detuning value helps for the efficiency of the teleportation. In this case, the values of the minimal

fidelity are decreased and infinitely close to zero with time. This means that the protocol for the entanglement channel of  $|\Psi^{0,3}\rangle$  is much better in the non-Markovian environment.

## V. CONCLUSION

The dynamics of the average fidelity for the standard teleportation is studied when the quantum channel is subject to the decoherence from the non-Markovian reservoirs. For the long time limit, the minimal fidelity is used to quantify the efficiency of the teleportation protocol. We also investigate the effects of the non-Markovianity of the channel on the teleportation. It is also found out that the memory effects can cause the revivals of the average fidelity and minimal fidelity. Compared with the Markovian environment, the scheme of the teleportation in the non-Markovian environment is much better because of the flowing of information from the environment back to the communication channel.

## Acknowledgement

It is a pleasure to thank Yinsheng Ling, Jianxing Fang for their many fruitful discussions about the topic. The work was supported by the Natural Science Foundation of China Grant No. 10904104 and No. 11074184.

- 
- [1] D. Loss and D. P. DiVincenzo, *Phys. Rev. A* **57** (1998) 120.
  - [2] M. A. Nielsen and I. L. Chuang, *Quantum Computation and Quantum Information*(Cambridge University Press, Cambridge, UK, 2000).
  - [3] H. P. Breuer and F. Petruccione, *The Theory of Open quantum Systems*(Oxford University Press, Oxford, UK, 2002).
  - [4] C. W. Gardiner and P. Zoller, *Quantum Noise*(Springer-Verlag, Berlin, 1999).
  - [5] C. H. Bennett, G. Brassard, C. Crepeau, R. Jozsa, A. Peres and W. K. Wootters, *Phys. Rev. Lett.* **70** (1993) 1895.
  - [6] J. Lee and M. S. Kim, *Phys. Rev. Lett.* **84** (2000) 4236.
  - [7] G. Bowen and S. Bose, *Phys. Rev. Lett.* **87** (2001) 267901.
  - [8] S. Albeverio, S. M. Fei and W. L. Yang, *Phys. Rev. A* **66** (2002) 012301.
  - [9] Y. Yeo and W. K. Chua, *Phys. Rev. Lett.* **96** (2006) 060502.



- [10] Y. Yeo, Phys. Rev. A **66** (2002) 062312.
- [11] Y. Yeo, Phys. Lett. A **309** (2003) 215.
- [12] Y. Yeo, Phys. Rev. A **68** (2003) 022316.
- [13] Y. Yeo, T. Q. Liu, Y. E. Lu and Q. Z. Yang, J. Phys. A: Math. Gen. **38** (2005) 3235.
- [14] C. X. Li, C. Z. Wang and G. C. Guo, Opt. Commun. **260** (2006) 741.
- [15] G. F. Zhang, Phys. Rev. A **75** (2007) 034304.
- [16] X. Hao and S. Zhu, Phys. Lett. A **338** (2005) 175.
- [17] S. Oh, S. Lee and H. W. Lee, Phys. Rev. A **66** (2002) 022316.
- [18] E. Jung, M. R. Hwang, Y. H. Ju, et. al., Phys. Rev. A **78** (2008) 012312.
- [19] D. D. Bhaktavatsala Rao, P. K. Panigrahi, C. Mitra, Phys. Rev. A **78** (2008) 022336.
- [20] J. Piilo, S. Maniscalco, K. Harkonen and K. A. Suominen, Phys. Rev. Lett. **100** (2008) 180402.
- [21] H. P. Breuer and J. Piilo, Europhys. Lett. **85** (2009) 50004.
- [22] X. L. Huang, H. Y. Sun and X. X. Yi, Phys. Rev. E **78** (2008) 041107.
- [23] F. F. Fanchini, T. Werlang, C. A. Brasil, L. G. E. Arruda and A. O. Caldeira, Phys. Rev. A **81** (2010) 052107.
- [24] B. Bellomo, R. Lo Franco and G. Compagno, Phys. Rev. Lett. **99** (2007) 160502.
- [25] J. G. Li, J. Zou and B. Shao, Phys. Rev. A **82** (2010) 042318
- [26] J. J. Chen, J. H. An, Q. J. Tong, H. G. Luo and C. H. Oh, Phys. Rev. A **81** (2010) 022120.
- [27] M. M. Wolf, J. Eisert, T. S. Cubitt and J. I. Cirac, Phys. Rev. Lett. **101** (2008) 150402.
- [28] H. P. Breuer, E. M. Laine and J. Piilo, Phys. Rev. Lett. **103** (2009) 210401.
- [29] Z. Y. Xu, W. L. Yang, and M. Feng, Phys. Rev. A **81**, (2010) 044105.

## Figure Captions

### Figure 1.

The dynamics of the optimized average fidelity  $F(t)$  is plotted as a function of the scaled time  $\gamma_0 t$  when the initial channel state is  $\rho^c(0) = |\Psi^{(0,3)}\rangle\langle\Psi^{(0,3)}|$ . In the Markovian regime of  $\lambda = 5\gamma_0$ , the solid curve and dashed curve correspond to the case of  $\delta = 0$  and  $\delta = 5\gamma_0$ .

### Figure 2.

The dynamics of the optimized average fidelity  $F(t)$  is plotted as a function of the scaled time  $\gamma_0 t$  when the initial channel state is  $\rho^c(0) = |\Psi^{(0,3)}\rangle\langle\Psi^{(0,3)}|$ . In the non-Markovian regime of  $\lambda = 0.01\gamma_0$ , the solid curve, dashed one, dotted curve correspond to the case of  $\delta = 2\gamma_0$ ,  $\delta = \gamma_0$  and  $\delta = 0$ .

### Figure 3.

The dynamics of the optimized average fidelity  $F(t)$  is plotted as a function of the scaled time  $\gamma_0 t$  when the initial channel state is  $\rho^c(0) = |\Psi^{(1,2)}\rangle\langle\Psi^{(1,2)}|$ . In the Markovian regime of  $\lambda = 5\gamma_0$ , the solid curve and dashed curve correspond to the case of  $\delta = 0$  and  $\delta = 5\gamma_0$ .

### Figure 4.

The dynamics of the optimized average fidelity  $F(t)$  is plotted as a function of the scaled time  $\gamma_0 t$  when the initial channel state is  $\rho^c(0) = |\Psi^{(1,2)}\rangle\langle\Psi^{(1,2)}|$ . In the non-Markovian regime of  $\lambda = 0.01\gamma_0$ , the solid curve, dashed one, dotted curve correspond to the case of  $\delta = 2\gamma_0$ ,  $\delta = \gamma_0$  and  $\delta = 0$ .

### Figure 5.

The dynamics of the minimal fidelity  $f(t)$  for the initial channel state of  $\rho^c(0) = |\Psi^{(0,3)}\rangle\langle\Psi^{(0,3)}|$  is plotted as a function of the scaled time  $\gamma_0 t$  when  $\lambda = 0.01\gamma_0$ . The solid line denotes the detuning value of  $\delta = 0$ . The dashed line represents the case of  $\delta = \gamma_0$ .

### Figure 6.

The dynamics of the minimal fidelity  $f(t)$  for the initial channel state of  $\rho^c(0) = |\Psi^{(1,2)}\rangle\langle\Psi^{(1,2)}|$  is plotted as a function of the scaled time  $\gamma_0 t$  when  $\lambda = 0.01\gamma_0$ . (a) The detuning value  $\delta = 0$ . (b) The detuning value  $\delta = \gamma_0$ .

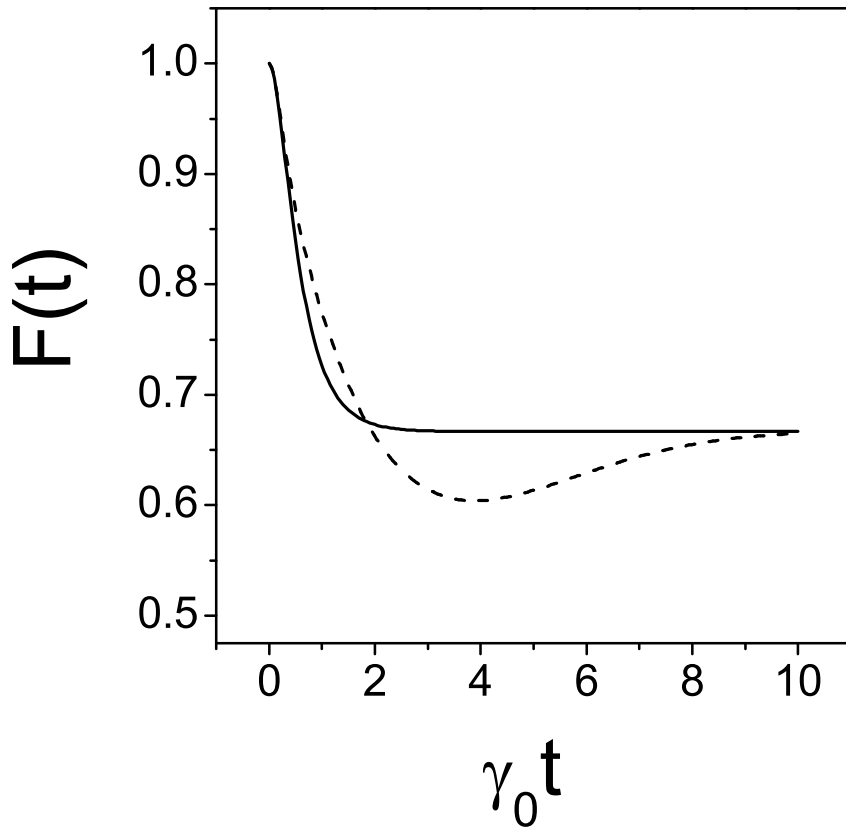


Figure 1

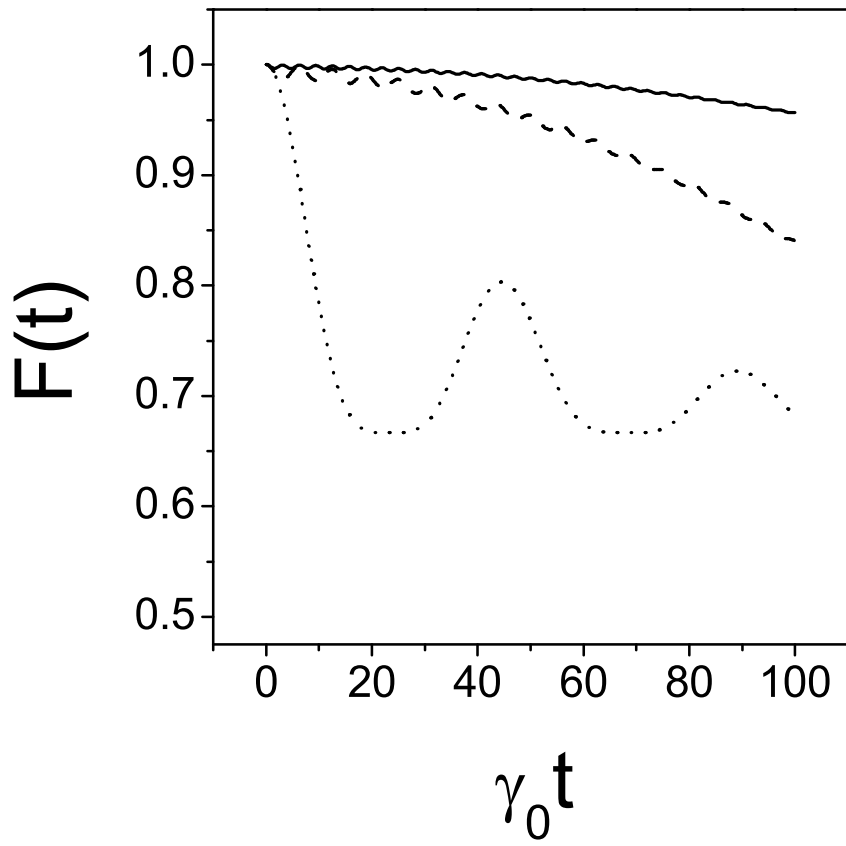


Figure 2

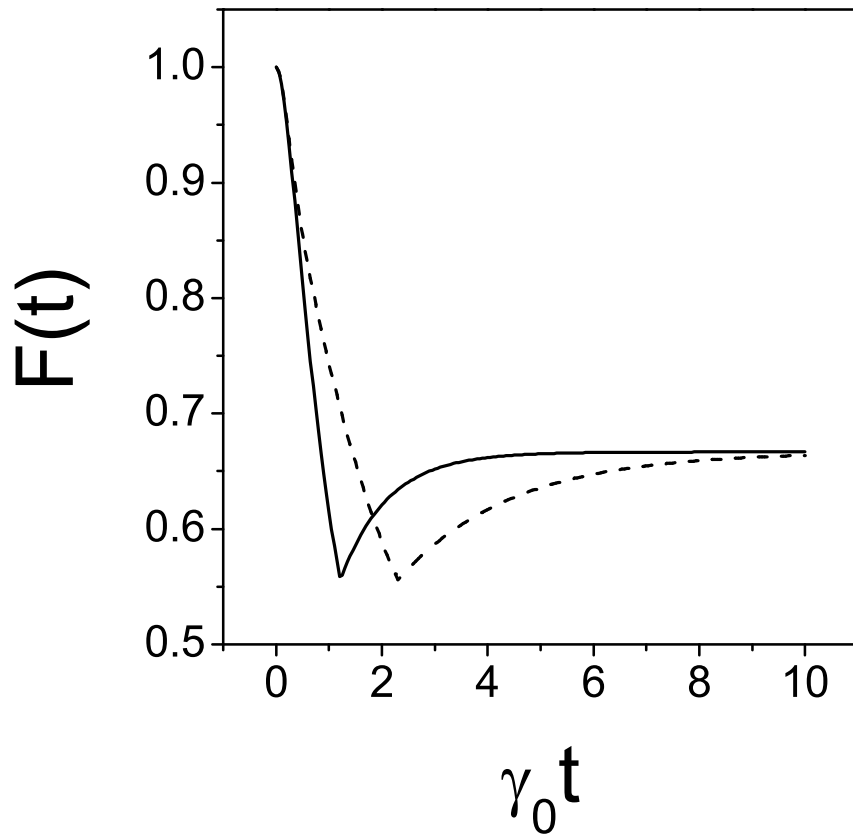


Figure 3

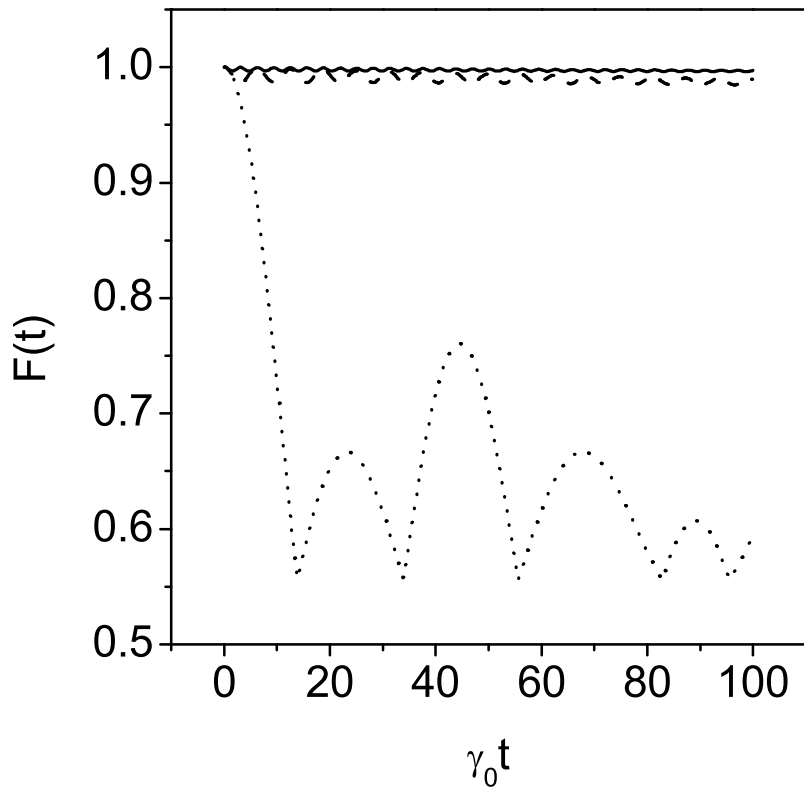


Figure 4

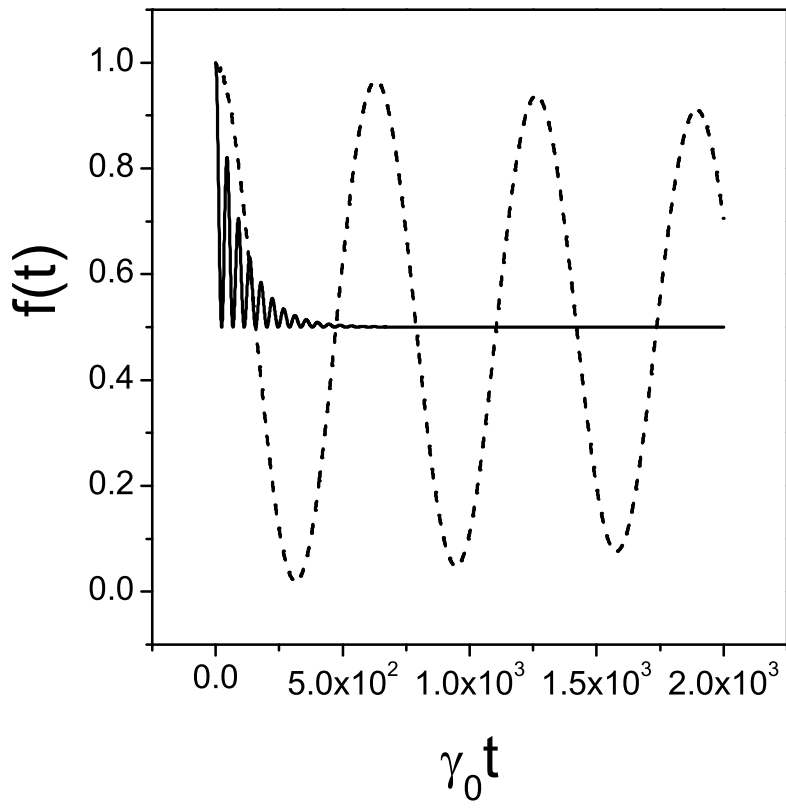


Figure 5

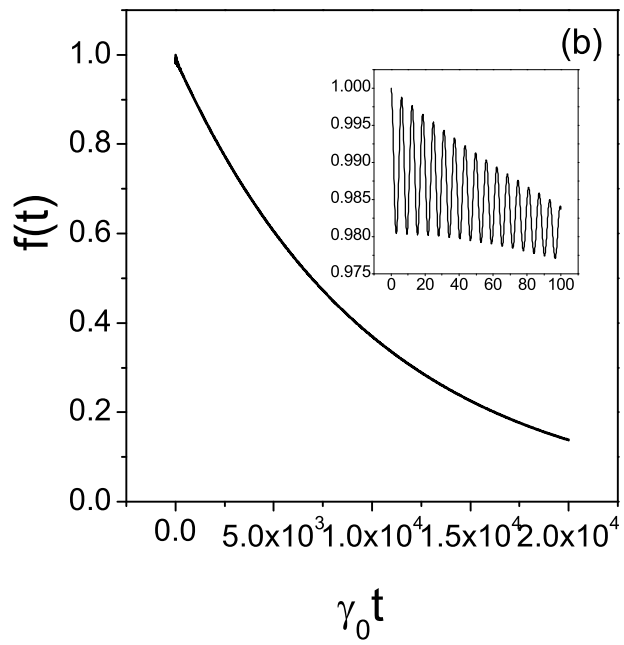
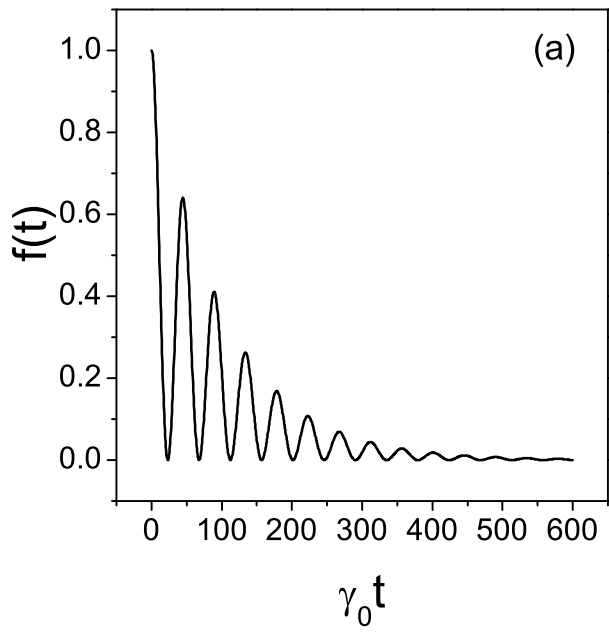


Figure 6